euspen's 16th International Conference & Exhibition, Nottingham, UK, May 2016
www.euspen.eu

Form error assessment of circular-arc cams

Shan Lin[1,2] , Otto Jusko[1], Frank Härtig[1] and Jörg Seewig[2]

[1] *Physikalisch-Technische Bundesanstalt, Bundesallee 100, 38116 Braunschweig, Germany*
[2] *Institute for Measurement and Sensor-Technology, Technical University of Kaiserslautern, Gottlieb-Daimler-Straße, 67663 Kaiserslautern, Germany*

shan.lin@ptb.de

Abstract
Precession cam profile of a camshaft has a significant effect on the performance of combustion engine. In order to evaluate the form error of a circular-arc cam, a global cam fitting algorithm based on the nonlinear least squares method is proposed for two probing strategies, e.g. ball probe and flat probe. The parameters of form, rotation, position are estimated iteratively by the Levenberg - Marquardt algorithm. The uncertainties associated with these parameters are estimated by the Monte Carlo simulation. For different probing strategies, both the uncertainties and the form errors are statistically compared.

Cam evaluation, least squares fitting, Monte Carlo simulation, uncertainty evaluation

1. Introduction

For a circular-arc cam evaluation, a conventional method is to separately estimate the form error for each circular arc, which is the local cam fit (LCF). However, it may cause discontinuity at the tangent points of two consecutive segments. In this paper, a global cam fitting algorithm (GCF) based on the least squares method is proposed. By taking geometric constraints into account, the continuity at tangent points is guaranteed. In form measurement of cam profile, ball probe and flat probe are widely applied on the coordinate or shaft measuring machines. Therefore, the GCF is derived correspondingly for the two probing strategies.

2. Mathematical description of circular-arc cam and its probe trace

2.1. Design a circular-arc cam profile

Parameters. A four circular-arc cam in a plane is described with eight parameters, as shown in Figure 1 (a), the radii r_b, r_t, r_{fr}, r_{fl} of four arcs, the center distance l of circular arcs Γ_1 and Γ_3, the rotation angle θ, and the center coordinates X_o, Y_o. Therefore, the cam model parameters $\mathbf{p}$ can be grouped and estimated in terms of form parameters $\mathbf{p_f}$, rotation parameter $\mathbf{p_r}$, and position parameters $\mathbf{p_p}$.

$$\mathbf{p}^{\mathrm{T}} = \qquad = \qquad !,\theta$$

Function. The implicit function of a circular arc Γ_k in an ideal coordinate system (ICS) *oxy* is

$$f_k\left(\mathbf{x_i},\mathbf{p_k}\right) = \left\|\mathbf{x_i}-\mathbf{e_k}\right\| - r_k = 0, \quad i \in I_k, \quad k = 1,\ldots \tag{1}$$

where $\mathbf{x_i} = (x_i, y_i)^{\mathrm{T}} \in \mathbb{R}^2$ is the coordinate vector of a sampled point in the ICS. $\mathbf{e_k} = (e_{k1}, e_{k2})^{\mathrm{T}}$ is the center coordinate vector of Γ_k. r_k is the radius of Γ_k. I_k is the index set. $\mathbf{p_k}$ is the parameter vector of the k^{th} segment of the cam, here $\mathbf{p_k} = (r_k, e_{k1}, e_{k2})^{\mathrm{T}}$.

Constraints. The cam profile is a closed and smooth form, thus its function should be continuously differentiable, especially at the tangent points of two consecutive segments. According to the tangent condition of two circles, the geometric constraints can be obtained.

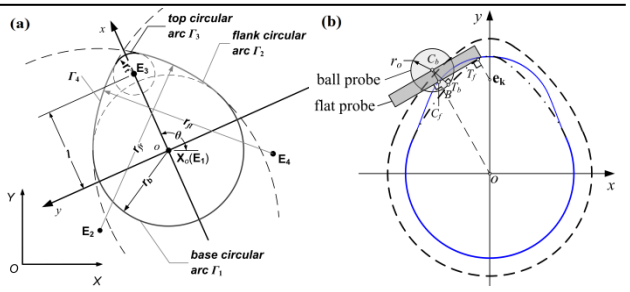

Figure 1. (a) A four circular-arc cam in a machine coordinate system *OXY* and an ICS *oxy*. (b) Nominal profile (dash-dot line), the trace of flat probe (solid line) and the trace of ball probe (dashed line) in an ICS.

2.2. Traced profile of probe

As shown in Figure 1 (b), the trace of ball probe center is obtained by dilating the nominal cam profile using the radius r_o of ball probe. The motion direction of flat probe is perpendicular to the tangent line of touching point.

Ball probe. The implicit function of a dilating circular arc Γ_k by the ball probe is

$$f_k\left(\mathbf{x_{bi}},\mathbf{p_k}\right) = \left\|\mathbf{x_{bi}}-\mathbf{e_k}\right\| - r_k - r_o = 0, \quad i \in I_k, \quad k = 1,\ldots \tag{2}$$

Flat probe. The implicit function of the trace of flat probe is

$$f_k\left(\mathbf{x_{fi}},\mathbf{p_k}\right) = \left\|\mathbf{x_{fi}}\right\|^2 - \mathbf{x_{fi}^{\mathrm{T}}}\mathbf{e_k} - r_k\left\|\mathbf{x_{fi}}\right\| = 0, \quad i \in I_k, \quad k = 1,\ldots \tag{3}$$

Eq. (2) and (3) are continuous and continuously differentiable at the connecting points of two consecutive segments. Therefore, the geometric constraints are the same as those in section 2.1.

3. Fitting algorithm

According to the nominal profile of cam, the nominal trace of probe is calculated. The form error is the difference between measured data and the nominal trace.

Except for the base circle, circular arcs are relatively short (smaller than half of a circle). The geometric fit is implemented by the nonlinear least squares method, which is to minimize the sum of the squares of the global geometric distance d_i under the geometric constraints.

$$\min_{\mathbf{p}} \sum_{k=1}^{K}\sum_{i=1}^{m} d_i^2 = \min_{\mathbf{p}} \sum_{k=1}^{K}\sum_{i=1}^{m} \min_{\mathbf{X_i'}} \left\|\mathbf{X_i}-\mathbf{X_i'}\right\|^2 \tag{4}$$

where $\mathbf{X_i'}=(X_i',Y_i')^{\mathrm{T}}$ is the coordinate vector of the minimum distance point on the model feature. These minimum distance points $\{\mathbf{X_i'}\}_{i=1}^{m}$ are alternately determined in a nested iteration scheme [1]. Levenberg - Marquardt algorithm [2] is adopted to solve the nonlinear least squares problem. The Jacobian matrix $\mathbf{J}_{d_i,\mathbf{p}}$ of the distance d_i is provided as follow.

Ball probe. The Jacobian matrix $\mathbf{J}_{d_i,\mathbf{p}}$ of d_i is given by

$$\mathbf{J}_{d_i,\mathbf{p}}=-\frac{(\mathbf{X_i}-\mathbf{E_k})^{\mathrm{T}}}{\|\mathbf{X_i}-\mathbf{E_k}\|}\left(\mathbf{R}^{-1}\frac{\partial \mathbf{e_k}}{\partial \mathbf{p_f}}\;\middle|\;\begin{matrix}-e_{k1}\sin\theta-e_{k2}\cos\theta\\ e_{k1}\cos\theta-e_{k2}\sin\theta\end{matrix}\;\middle|\;\mathbf{I}_2\right) -\left(\frac{\partial r_k}{\partial \mathbf{p_f}}\;\middle|\;\mathbf{0}_{1,3}\right) \tag{5}$$

Flat probe. The Jacobian matrix $\mathbf{J}_{d_i,\mathbf{p}}$ of d_i is given by

$$\mathbf{J}_{d_i,\mathbf{p}}=\left(-\frac{sign\left((\mathbf{x_i}-\mathbf{x_i'})^{\mathrm{T}}\nabla f_k\right)}{\|\nabla f_k\|}\left(\mathbf{x}^{\mathrm{T}}\mathbf{R}^{-1}\frac{\partial \mathbf{e_k}}{\partial \mathbf{p_f}}+\|\mathbf{x}\|\frac{\partial r_k}{\partial \mathbf{p_f}}\right)\Bigg|_{\mathbf{x}=\mathbf{x_i'}}\;\middle|\;\mathbf{0}_{1,3}\right) \tag{6}$$
$$-\frac{(\mathbf{X_i}-\mathbf{X_i'})^{T}}{\|\mathbf{X_i}-\mathbf{X_i'}\|}\left(\mathbf{0}_{2,5}\;\middle|\;\begin{matrix}-x_i'\sin\theta-y_i'\cos\theta\\ x_i'\cos\theta-y_i'\sin\theta\end{matrix}\;\middle|\;\mathbf{I}_2\right)$$

4. Numerical validation

The effectiveness of the proposed algorithms is validated by numerical experiments. To simulate a nominal profile, a four circular-arc cam is adopted [3]: r_b = 18 mm, r_t = 5 mm, r_{fr} = 43 mm, r_{fl} = 43 mm, l = 20 mm.

4.1 Effect of random error

According to Eq. (1) - (3), three data sets $\{\mathbf{x_i}\}_{i=1}^{360}$, $\{\mathbf{x_{bi}}\}_{i=1}^{360}$ and $\{\mathbf{x_{fi}}\}_{i=1}^{360}$ are taken as nominal points (sampling interval 1°) by ball probe (r_o = 0 mm, r_o = 1.5 mm) and flat probe, respectively. Gaussian noise (σ_0 = 1 μm) is superimposed on the nominal points. The LCF and GCF are implemented to estimate the parameters **p** respectively. The mean average error (MAE), the root-mean-square error (RMSE) and the peak-to-valley (PV) are calculated for comparison of error. The process is repeated for 1000 times and the distributions of the obtained parameters are presented in Table 1.

Table 1 The expanded uncertainties U (k = 2) of the fitted parameters and the distributions of form errors.

	ball probe				**flat probe**
	r_o = 0		**r_o = 1.5 mm**		
	LCF	**GCF**	**LCF**	**GCF**	**GCF**
$U(r_b)$/μm	0.183	0.166	0.183	0.169	0.181
$U(r_t)$/μm	7.215	4.152	11.875	3.854	3.125
$U(r_{fr})$/μm	29.173	19.158	27.106	18.999	19.187
$U(r_{fl})$/μm	29.085	19.062	25.711	18.351	19.624
$U(l)$/μm	7.766	4.776	12.489	4.402	3.396
$U(\theta)$/°	4.18e-03	2.44e-03	4.88e-03	2.01e-03	9.54e-04
$U(X_o)$/μm	0.294	0.260	0.290	0.267	0.134
$U(Y_o)$/μm	0.168	0.162	0.174	0.165	0.083
MAE/μm	0.784	0.790	0.821	0.776	0.790
U(MAE)/μm	0.058	0.065	0.064	0.060	0.062
RMSE/μm	0.971	0.989	1.075	0.973	0.989
U(RMSE)/μm	0.070	0.077	0.081	0.070	0.073
PV/μm	5.763	5.843	10.824	5.725	3.124
U(PV)/μm	1.068	1.068	2.059	1.033	0.683

Compared to the LCF, the reduction of uncertainty in each parameter is apparent in the GCF for ball probe. The results of MAE and RMSE are similarly distributed for different probes. However, the value of PV and its standard deviation of flat probe are smaller than those of ball probe, indicating that the flat probe tends to underestimate the form error.

4.2 Effect of systematic form error

Systematic form deviation [4] is superimposed on the nominal points $\{\mathbf{x_i}\}_{i=1}^{3600}$. The form error e_o is determined by the GCF for ball probe (r_o = 0) and treated it as the 'true' form error. Select m = 36, 72, 180, 360 data points $\{\mathbf{x_i}\}_{i=1}^{m}$ from the 3600 points by the Latin hypercube sampling, and treat them as touching points. The sample process repeats 100 times. According to the touching points, probe positions $\{\mathbf{x_{bi}}\}_{i=1}^{m}$ and $\{\mathbf{x_{fi}}\}_{i=1}^{m}$ are calculated using the morphological operations [5]. Then the GCF is employed for different probing strategies to obtain the form error. The ratios $\hat{e}(m)/e_o$, $\hat{e}_b(m)/e_o$, $\hat{e}_f(m)/e_o$ are calculated and shown in box-whiskers in Figure 2.

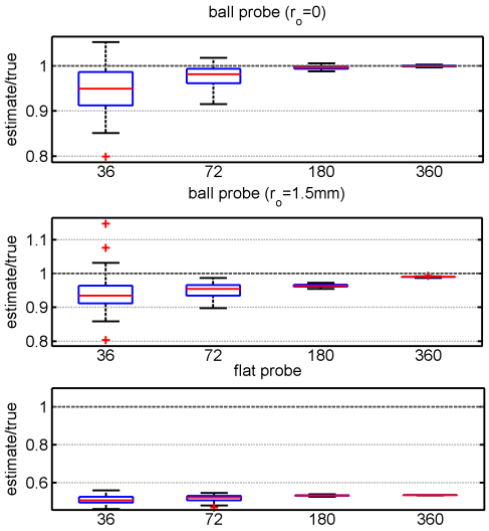

Figure 2. Results of form error estimation estimate for different probes.

When the sample size grows larger, the results for ball probe (r_o = 0 mm) tend to be unbiased. For r_o = 1.5 mm, the ratios approach to one with a relatively large sample size. However, the form error measured by flat probe is around 50% smaller than true value, even in large sample size.

5. Conclusion

A GCF approach was proposed to evaluate the form error of the circular-arc cam for different probing strategies. Compared to a conventional method, the uncertainties associated with the estimated parameters by the GCF are lower. For ball probe, the form error approach to the true value with smaller radius and large sample size. However, the form error estimated by flat probe is about 50% smaller than the true value.

References

[1] Sung Joon Ahn, Wolfgang Rauh, Hyung Suck Cho, Hans-Jürgen Warnecke 2002 *IEEE Trans Pattern Anal Mach Intell* **24** 5 620-638

[2] Jorge J. Moré 1978 *Numerical Analysis* **630** 105-116

[3] Künne, Bernd 2008 *Köhler/Rögnitz Maschinenteile 2*

[4] Mesay T. Desta, Hsi-Yung Feng and Daoshan OuYang 2003 *Int. J. Mach. Tool Manu.* **40** 11 1069-1078

[5] Jagadeesha Kumar and Shunmugam MS 2006 *Int. J. Mach. Tool Manu.* **46** 3 260-270